Supporting Information

Strong-Alkali Resistant Zinc-Organic Framework with 1,3,6,8-tetra(pyridin-4-yl)pyrene for Efficiently Photocatalytic Hydrogen Evolution

Guo-Li Yang[a,b], Yao Xie[a], Zhuo-Hao Jiao[a], Jian Zhao[a], Sheng-Li Hou[a], Ying Shi[a], Jie Han[a], and Bin Zhao[a]**

[a] Department of Chemistry, Key Laboratory of Advanced Energy Marerial Chemistry, MOE, and Collaborative Innovation Center of Chemical Science and Engineering, Nankai University, Tianjin 300071

[b] Department of Chemistry and Chemical Engineering, Jinzhong University, Jinzhong, 030619, China.

Table of Contents

Section A:

Materials

All reagents in this work were obtained from commercial sources and utilized without furthermore purification, and deionized water was used throughout the experimental part. Zinc acetate ($Zn(OAc)_2 \cdot 2H_2O$, 98%), Hydrochloric(HCl, 99%), Nitric acid (HNO_3, 99%), Methanol (CH_3OH), Potassium carbonate (K_2CO_3), Triethanolamine (TEOA), N-Methyl Pyrrolidone (NMP), 1,4-Dioxane (DOA) were purchased from Sinopharm Chemical Reagent Co. Ltd. Tetrakis(triphenylphosphine)palladium ($Pd(pph)_3)_4$), 4-Pyridylboronic acid (Py-4-boron), and 1,3,6,8-tetrabromopyrene were purchased from Hengshan chemical.

General Methods

Powder X-ray diffraction (PXRD) patterns with Cu-Kα incident radiation by Ultima IV X-ray diffractometer and D/Max-2500X instrument. Fourier transform infrared spectra (IR) was performed at Bruker Vector 22 spectrometer. Elemental analysis (EA) was measured by the Bruker Vector 22 spectrometer instrument. Thermogravimetric analyses (TGA) experiments were performed on Netzsch TG 209 TG-DTA analyzer. UV-Vis absorption was recorded on the HITACHI U-3900 and JASCOV-570 spectrometer. Scanning Electron Microscope (SEM) images were obtained on HITACHI S-4800. Transmission electron microscopy (TEM) images were performed with FEI Tecnai (F30 G2, Twin). Photocatalytic measurements were determined on the labsolar 6A analyzer. electrochemical measurements were determined on an electrochemical analyzer (CHI 660E). Photoluminescence spectra were measured on a HITACHI F-4600 instrument.

Crystallography

The crystal structures were determined at 296(2) K by a Bruker SMART 1000, Oxford SuperNova TM diffractometer with graphitemono chromatic Mo Kα radiation source (λ = 0.71073 Å). The structure was solved and refined by direct methods SHELXS-97 and SHELXL-97 programs. The H atoms fixed to their geometrically ideal positions were refined isotropically by full-matrix least-squares methods.[1] Their

electronic contributions are eliminated by the SQUEEZE manipulation in PLATON.[2] The refinement results are provided in Table S1.

Section B:

Samples preparation

All purified samples remain to keep in mother liquor before experiment with the synthesis process in main text. The sample for electrochemical measurement was prepared by FTO section with loaded sample powders. The detailed procedures as follows: 5 mg of sample was grinded and suspended in the mixture solution (containing 700 μL H_2O, 270 μL acetone and 15 μL Nafion aqueous), ultrasonication until dispersion uniformly. After that, the resulting colloidal dispersion (10 μL) repeatedly was dropped onto the conductive glass with the proportion of 1×1 cm^2.

Electrochemical Measurements

Electrochemical measurements were carried out in a standard three-electrode system with the dried MOF-coated FTO working electrode, a Pt foil counter electrode, and a saturated calomel electrode (SCE) reference electrode. The FTO electrodes were dried in air for 3h at room temperature. The electrolyte was 0.2 M phosphate buffer solution with a pH value of 7.0. The M-S measurement was carried out using an electrochemical analyzer (CHI 660E) and the frequency was 1 kHz. Photoelectrochemical measurements were carried out in a standard three-electrode system, with the MOF-coated FTO working electrode, a Pt foil counter electrode, and a saturated calomel electrode (SCE) reference electrode. The electrolyte was 0.2 M phosphate buffer solution with a pH value of 7.0.

Photocatalytic Hydrogen Production Experiment

The photocatalytic hydrogen production process was carried out with a photocatalytic device manufactured by labsolar 6A analyzer with a 300W Xe lamp (380 nm $\leq \lambda \leq$ 780 nm) as the light source. Photocatalytic reactions were performed in a 100 mL quartz reaction flask. 20 mg of samples were added into the prepared mixture of the sacrificial agent TEOA (10 vol%) and the co-catalyst chloroplatinic acid $H_2PtCl_6 \cdot 6H_2O$ (5 wt%). After sealing the reactor by the septum, this suspension was

continuously degassed by argon for 30 min. The Xe lamp was used to irradiate the above suspension connected to the circulating condensation water. Besides, The GC-7900T Techcomp instrument was used to monitor and record the amount of H_2 in real-time.

Measurement of apparent quantum efficiency

The apparent quantum efficiency (AQE) was measured by a quantum yield measurement system (PLR-QY1000, Beijing Perfectlight Technology Co., Ltd.) with a laser light source (408 nm ± 10 nm). The AQE was calculated as following:

$$\mathrm{AQE} = \frac{2r}{I} \times 100\%$$

Where, $\boldsymbol{r}$ represents the evolution rate of H_2 in the initial one hour irradiation. $\boldsymbol{I}$ represents the number of photons reaching the reaction solution.

Calculation method

All the density-functional theory (DFT) computations were performed using the Cambridge Sequential Total Energy Package (CASTEP) based on the pseudopotential plane wave (PPW) method. Electron-ion interactions were described using the ultrasoft potentials (USP). A plane-wave basis set was employed to expand the wave functions with a cutoff kinetic energy of 400 eV. For the electron-electron exchange and correlation interactions, the functional parametrized by Perdew-Burke-Ernzerhof (PBE), a form of the general gradient approximation (GGA), was used throughout with the Hubbard U set to 4.7 eV for Zn for the better description of exchange-correlation interaction. The Vander Waals interaction was described using the DFT-D2 method that proposed by Grimme.

During the geometry optimizations, all the atom positions were allowed to relax. In this work, the Brillouin-zone integrations were conducted using Monkhorst-Pack (MP) grids of special points with the separation of 0.07 $Å^{-1}$ for the model cell. The convergence criterion for the electronic self-consistent field (SCF) loop was set to 10^{-5} eV/atom. The atomic structures were optimized until the residual forces were below 0.03 $eVÅ^{-1}$.

Section C:

Figures S1-19

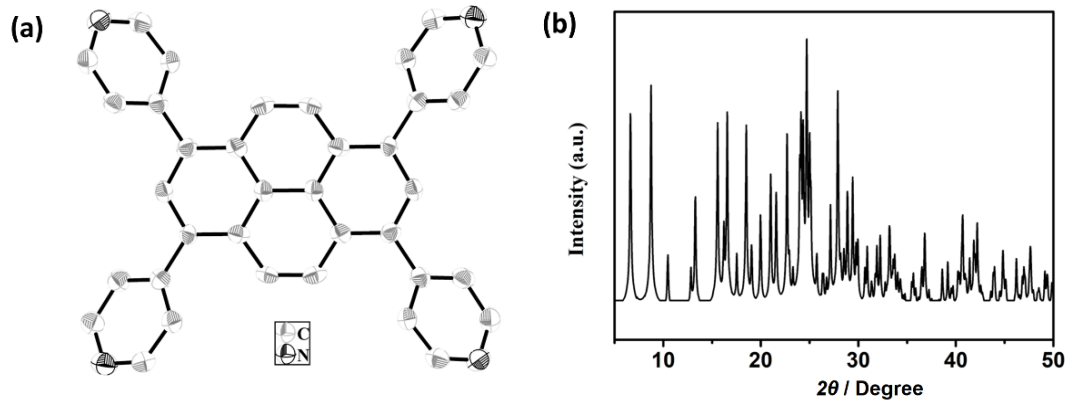

Figure S1. (a) The structure of the ligand TTPy; (b) the simulated PXRD of the ligand TTPy

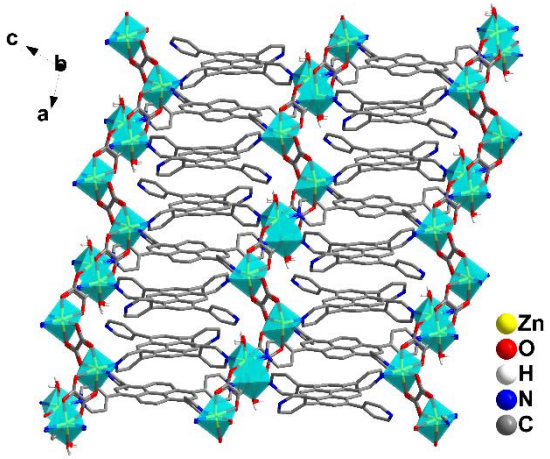

Figure S2. The 2D layered structure of **1** along b direction, which displays two types of modes for ligand TTPy.

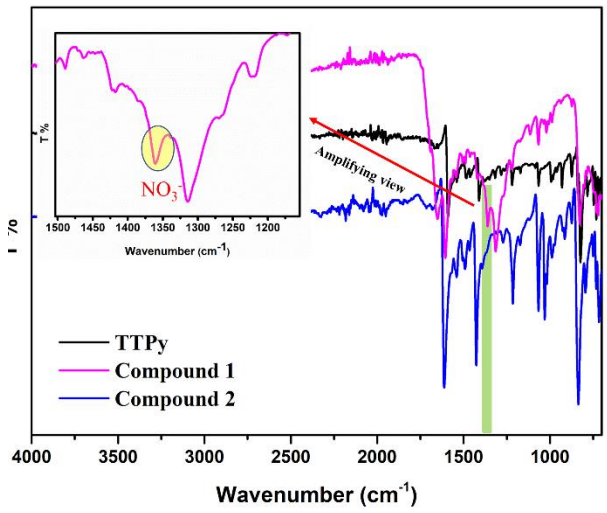

Figure S3. FT-IR curves of ligand TTPy, compounds **1** and **2**.

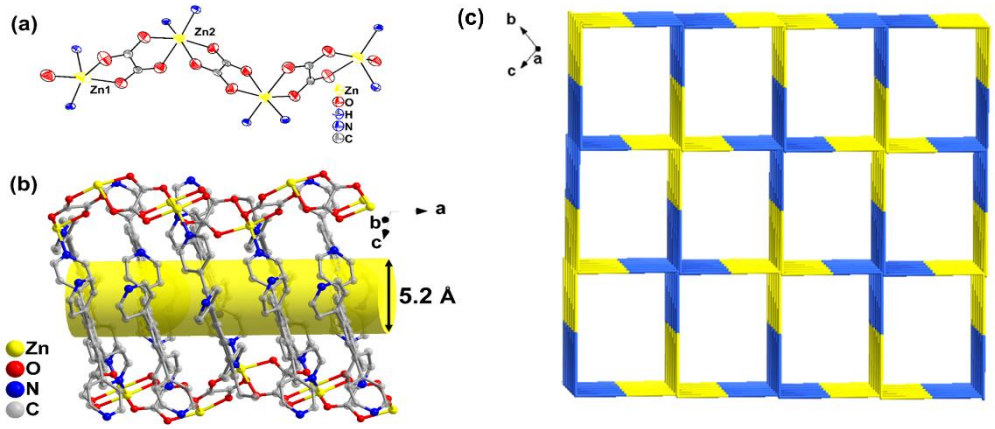

Figure S4. (a) The coordination environment of metal ion Zn(II). (b) The skeleton of compound **1** with channels approximately 5.2 Å by ball-stick mode. (c) Simplified topology network of compound **1**.

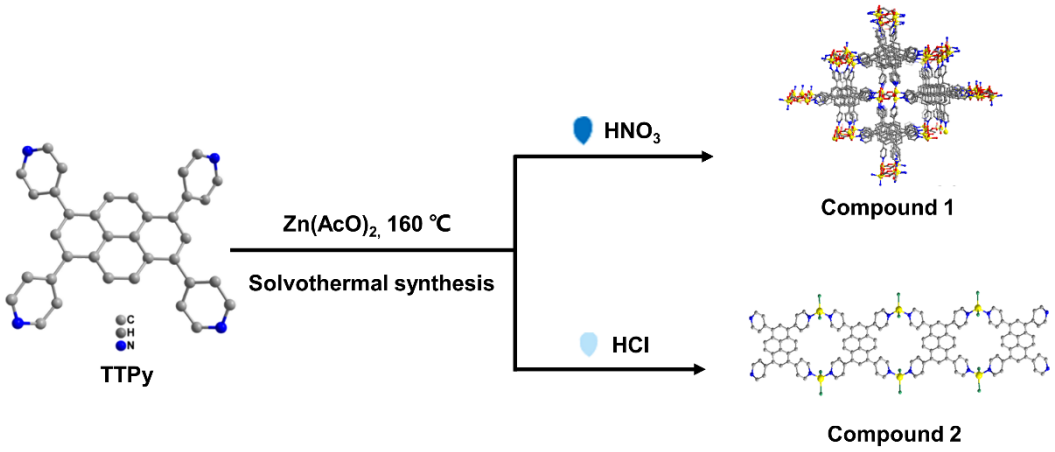

Figure S5. The synthesis route of compounds **1** and **2**.

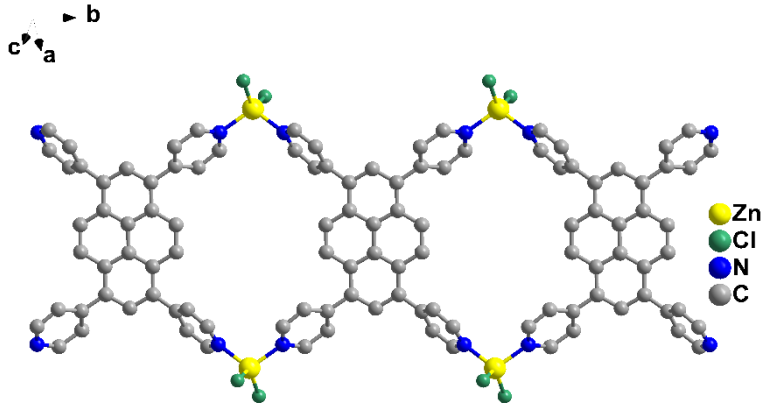

Figure S6. 1D chain structure of compound **2**.

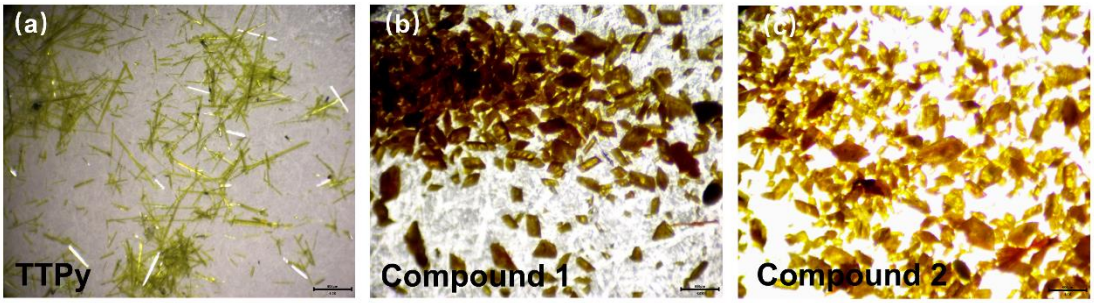

Figure S7. The microscope images of ligand TTPy, compounds **1** and **2**.

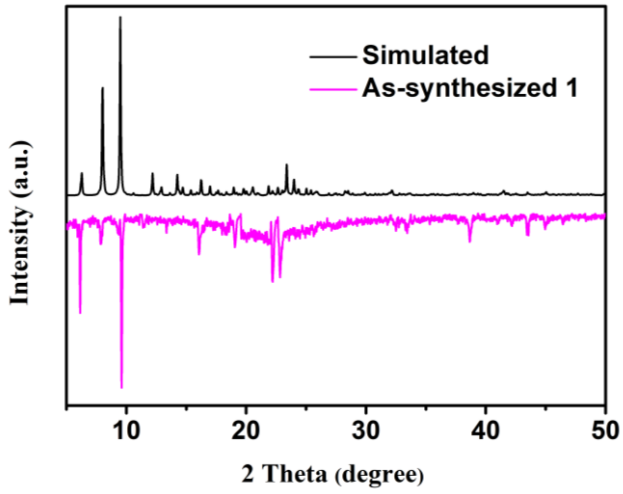

Figure S8. As-synthesized and simulated PXRD patterns for compound **1**.

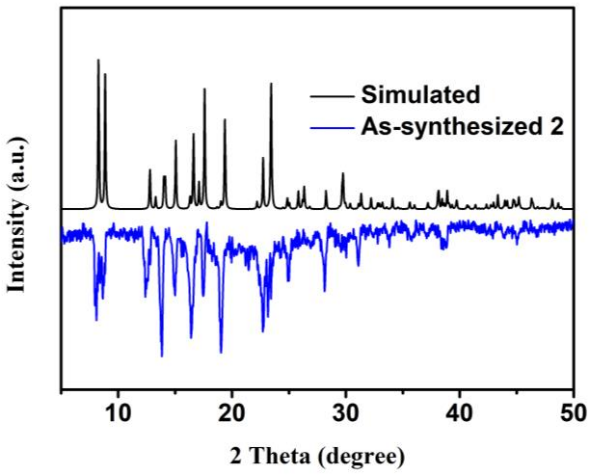

Figure S9. As-synthesized and simulated patterns for compound **2**.

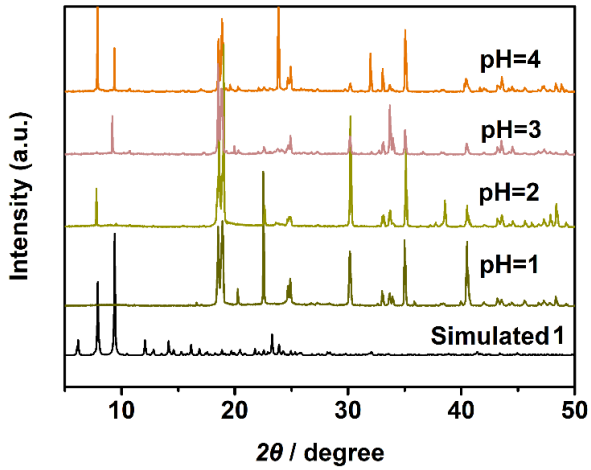

Figure S10. PXRD patterns of as-synthesized **1** in the solutions with pH = 1-4.

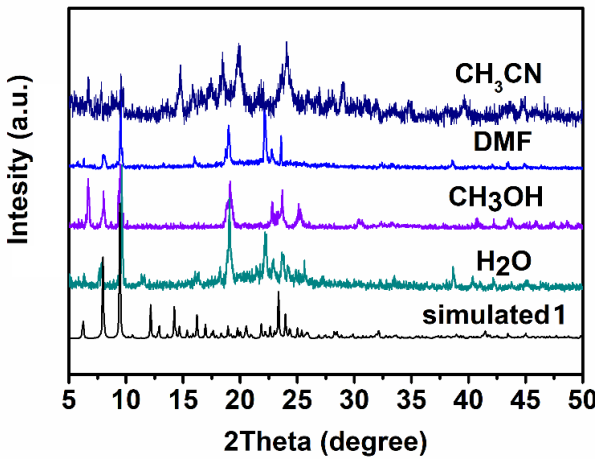

Figure S11. PXRD pattern of the as-synthesized **1** in common organic solvents.

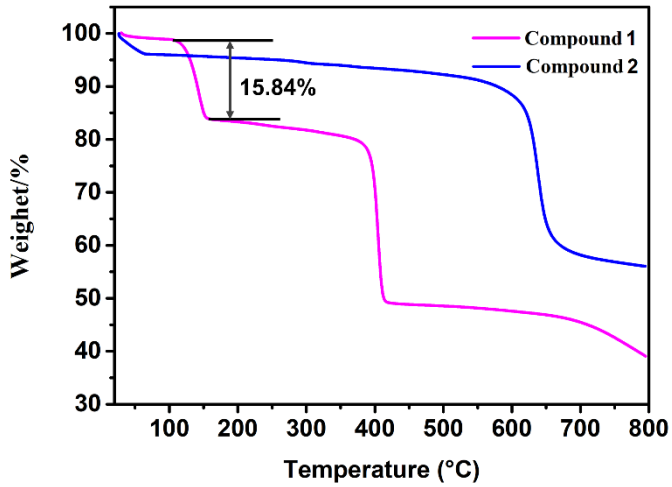

Figure S12. TG curves of compounds **1** and **2**.

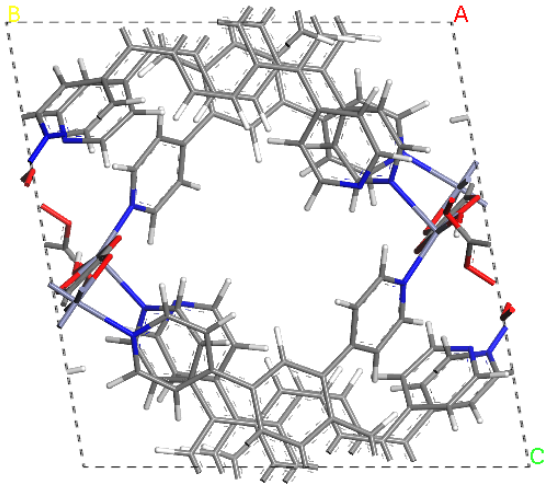

Figure S13. The optimized structure model of compound **1**.

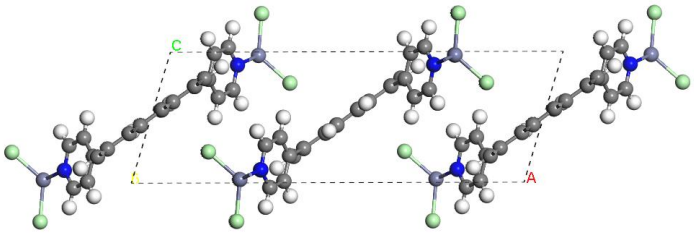

Figure S14. The optimized structure model of compound **2**.

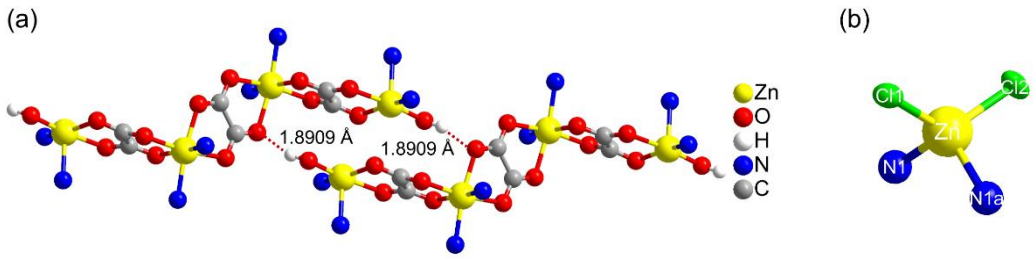

Figure S15. The coordination environments of Zn node for compound **1** (a) and **2** (b).

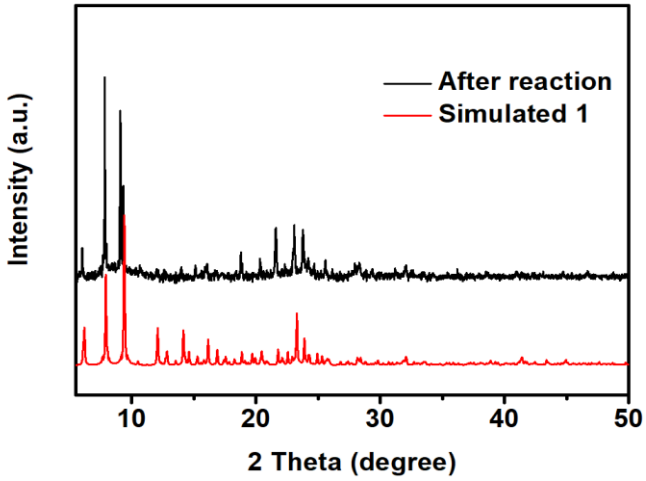

Figure S16. PXRD pattern of **1** before and after photocatalytic experiments.

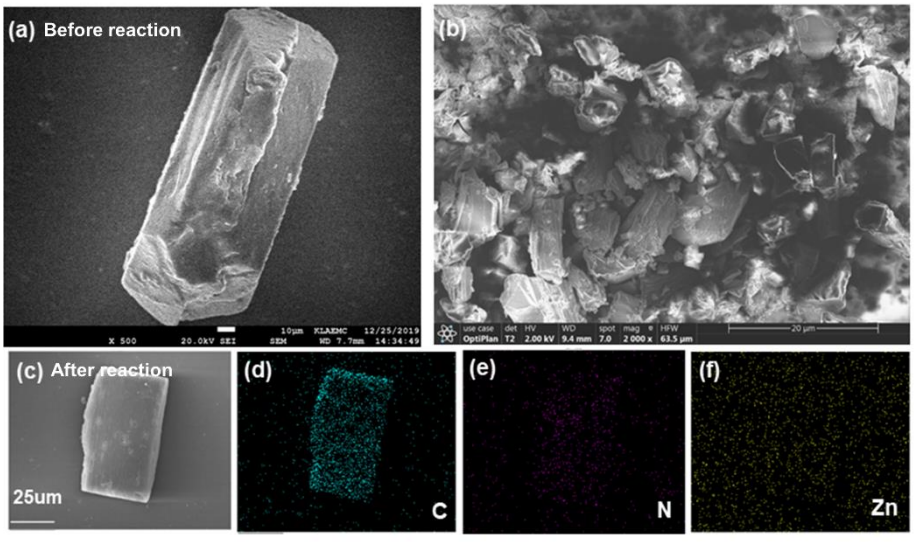

Figure S17. SEM images and element mapping images of **1** before and after photocatalysis reaction.

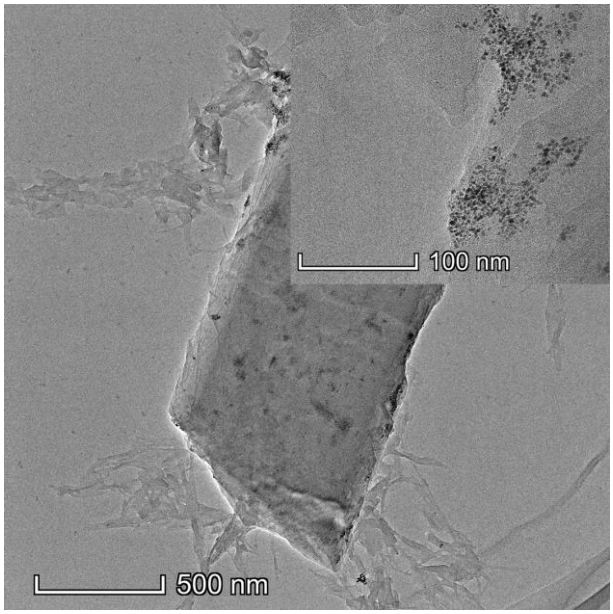

Figure S18. TEM images of compound **1** after reaction.

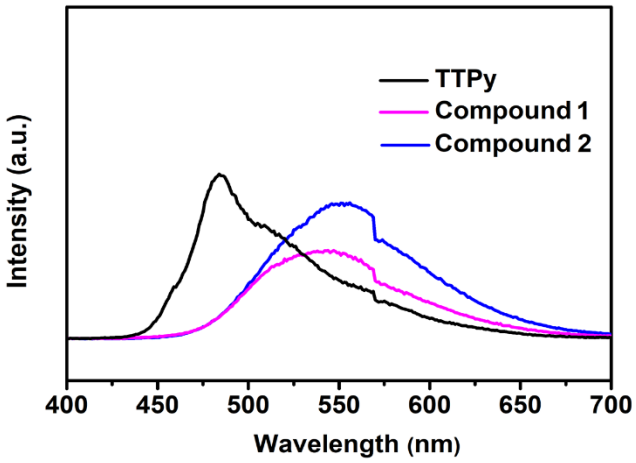

Figures S19. Steady-state emission spectra of compounds **1** and **2**.

Section D:

Tables S1-4

Table S1. Crystallographic data for TTPy, compounds **1** and **2**

Identification code	TTPy	1	1 in TEOA	2
Formula weight	195.56	1046.65	1046.65	391.56
***T* (K)**	120.00(10)	118.7(3)	154(17)	121(2)
Crystal system	triclinic	triclinic	triclinic	monoclinic
Space group	$P2_1/n$	$P\text{-}1$	$P\text{-}1$	$I2/m$
***a* (Å)**	3.94142(19)	12.2586(5)	12.2632(6)	7.2221(7)
***b* (Å)**	10.9293(5)	14.4889(6)	14.4805(12)	12.6213(14)
***c* (Å)**	26.6699(14)	15.5403(7)	15.5400(8)	19.960(2)
***α* (°)**	90	99.156(4)	99.417(6)	90
***β* (°)**	91.916(5)	108.857(4)	108.864(5)	93.454(10)
***γ* (°)**	90	90.364(4)	90.091(5)	90
***V* (Å^3)**	1148.22(10)	2573.8(2)	2571.7(3)	1816.1(3)
Z	5	2	2	4
$D_{calcd.}$[g·cm^{-3}]	1.1414	1.351	1.687	1.432
μ (mm^{-1})	0.086	0.990	2.586	1.645
F (000)	489.0	1070.0	1072.0	788.0
R_{int}	0.0235	0.0308	0.0804	0.0322
Goof	1.001	1.045	1.037	1.100
Final R indexes	R_1 = 0.0525	R_1 = 0.0432	R_1 = 0.0715	R_1 = 0.0756
[I>=2σ (I)]	wR_2 = 0.1444	wR_2 = 0.1049	wR_2 =0.1856	wR_2 = 0.1898
Final R indexes	R_1 = 0.0698	R_1 = 0.0593	R_1 = 0.1076	R_1 = 0.0899
[all data]	wR_2 = 0.1635	wR_2 = 0.1131	wR_2 = 0.2430	wR_2 = 0.2019

Table S2. MOFs as photocatalysts for hydrogen production in comparison

Photocatalysts	Bandgap	Sacrificial agent	Reaction time	Activity
This work	2.21	TEOA	35 h	315.06 μmol g^{-1} h^{-1}
ZIF-67 [3]	_	TEOA	10 h	48.5 μmol h^{-1}
ZIF-67 [4]	_	TEOA	48 h	843.7 μmol g^{-1} h^{-1}
P-ZIF-67 [5]	_	TEOA	5 h	63.4 μmol h^{-1}
UiO-66 [6]	3.05	MeOH	3 h	0.8 mL h^{-1}
ZIF-9[7]	_	TEOA	5 h	85.66 μmol h^{-1}
NH_2-UiO(Zr/Ti)-66 [8]	2.88	MeCN/TEOA	10 h	0.58 mmol h^{-1} mol^{-1}
$[Co_3(HL)_2 \cdot 4DMF \cdot 4H_2O]$[9]	2.95	DMF/H_2O	12 h	0.83 μmol h^{-1}

Zr-MOF-bpy-$PtCl_2$ [10]	2.69	TEOA	9 h	0.92 μmol h^{-1} g^{-1}
MIL-167 [11]	_	TEA	25 h	7.7 μmol h^{-1} g^{-1}
$[Al_3(OH)_3(HTCS)_2]$ [12]	2.59	TEOA	14 h	50 μmol h^{-1} g^{-1}
Pt@MIL-125/Au[13]	3.72	TEOA	100 h	1.74 mmol $h^{-1}g^{-1}$
Ti-MOF-Ru(tpy)$_2$ [14]	_	TEOA	3 h	1.82 μmol h^{-1}
Cu-I-bpy [15]	2.05	TEA	24 h	7.09 mmol $h^{-1}g^{-1}$
Cd-TBAPy [16]	2.15	TEOA	3 h	4.3 μmol h^{-1}
20%-MIL-125-$(SCH_3)_2$ [17]	2.69	TEOA	2 h	3.81 mmol g^{-1} h^{-1}
USTC-8(In) [18]	1.79	TEA	4 h	341.3 μmol g^{-1} h^{-1}
$[Zn_2(H_2O)_3\{PdCl_2(pydc)_2\}]_n$ [19]	_	EDTA-2Na	4 h	TON = 20.2
$[Dy_2(abtc)(H_2O)_2(OH)_2]_2H_2O$[20]	2.17	TEOA	5 h	21.53 μmol $h^{-1}g^{-1}$
$[Zn\{Pd(INA)_4\}]_n$ [21]	_	EDTA-2Na	4 h	TON = 28.2
CoNi@NH_2BDC [22]	2.2	CH_3OH	4 h	27.02 h^{-1} μmol
(PBA)-Ni [23]	_	TEOA	6 h	20.0 μmol h^{-1}

Table S3. The blank experiments for photocatalytic hydrogen production

Catalyst	Illumination	Sacrificial agent	Co-catalyst	H_2 production
$Zn(OAc)_2$	380 nm ≤ λ ≤ 780 nm	TEOA	$H_2PtCl_6·6H_2O$	_
TTPy	380 nm ≤ λ ≤ 780 nm	TEOA	$H_2PtCl_6·6H_2O$	_
$Zn(OAc)_2$, TTPy	380 nm ≤ λ ≤ 780 nm	TEOA	$H_2PtCl_6·6H_2O$	_
_	380 nm ≤ λ ≤ 780 nm	TEOA	$H_2PtCl_6·6H_2O$	_
Compound **1**	_	TEOA	$H_2PtCl_6·6H_2O$	_
Compound **1**	380 nm ≤ λ ≤ 780 nm	TEOA	_	_

Table S4. The ICP results of mixture filtrate after photocatalytic reaction (35h)

Filter liquor	The leakage of Zn^{2+}
After reaction 35h for photocatalytic experiment	0.11 **%**

Section E:

References

1. O. V. Dolomanov, L. J. Bourhis, R. J. Gildea, J. A. K. Howard, H. Pushmann, OLEX 2: a complete structure solution, refinement and analysis program. *J. Appl. Crystallogr*. 2009, **42**, 339-341.
2. A. L. Spek, PLATON, A multipurpose crystallographic tool. *Utrecht University: Utrecht, The Netherlands*. 2001.
3. S. Yang, B. Pattengale, E. L. Kovrigin, J. Huang, *ACS Energy Lett.* 2017, **2**, 75–80.
4. B. Pattengale, S. Yang, S. Lee, *ACS Catal.* 2017, **7**, 8446–8453.
5. Y. Li, Z. Jin, T. Zhao, *Chem. Eng. J.* 2020, **382**, 123051-123068.
6. C. G. Silva, I. Luz, F. X. Llabrés I Xamena, A. Corma, H. García, *Chem. A Eur. J.* 2010, **16**, 11133–11138.
7. H. Wang, Z. Jin, *Sustain. Energy Fuels* 2019, **3**, 173–183.
8. D. Sun, W. Liu, M. Qiu, Y. Zhang, Z. Li, *Chem. Commun.* 2015, **51**, 2056–2059.
9. W. M. Liao, J. H. Zhang, Z. Wang, Y. L. Lu, S. Y. Yin, H. P. Wang, Y. N. Fan, M. Pan, C. Y. Su, *Inorg. Chem.* 2018**, 57**, 11436–11442.
10. T. Toyao, M. Saito, S. Dohshi, K. Mochizuki, M. Iwata, H. Higashimura, Y. Horiuchi, M. Matsuoka, *Res. Chem. Intermed.* 2016, **42**, 7679–7688.
11. H. Assi, L. C. Pardo Pérez, G. Mouchaham, F. Ragon, M. Nasalevich, N. Guillou, C. Martineau, H. Chevreau, F. Kapteijn, J. Gascon, P. Fertey, E. Elkaim, C. Serre, T. Devic, *Inorg. Chem.* 2016, **55**, 7192–7199.
12. Y. Y. Guo, J. Zhang, L. Z. Dong, Y. Xu, W. Han, M. Fang, H.K. Liu, Y. Wu, Y.Q. Lan, *Chem. Eur. J.* 2017, **23***,* 15518–15528.
13. J. D. Xiao, L. L. Han, J. Luo, S.H. Yu, H. L. Jiang, *Angew. Chem. Int. Ed.* 2018**, 57***,* 1103–1107.
14. T. Toyao, M. Saito, S. Dohshi, K. Mochizuki, M. Iwata, H. Higashimura, Y. Horiuchi, M. Matsuoka, *Chem. Commun*. 2014, **50**, 6779–6781.
15. D.Y. Shi, R. Zheng, M.J. Sun, X.R. Cao, C.X. Sun, C.J. Cui, C.S. Liu, J.W. Zhao, M. Du, *Angew. Chem. Int. Ed*. 2017, **56***,* 14637–14641.
16. Y. J. Xiao, Y. Qi, X.L. Wang, X.Y. Wang, F.X. Zhang, C. Li, *Adv. Mater.* 2018, **30**, 1803401-1803408.
17. S.Y. Han, D.L. Pan, H. Chen, X.B. Bu, Y.X. Gao, H. Gao, Y. Tian, G.S. Li, G. Wang, S. L. Cao, C.Q. Wan, G.C. Guo, *Angew. Chem. Int. Ed*. 2018, **57**, 9864–9869.
18. F.C. Leng, H. Liu, M.L. Ding, Q.P. Lin, H.L. Jiang, *ACS Catal*. 2018, **8**, 4583–4590.
19. Y. Miyazaki, Y. Kataoka, W. Mori, J. Nanosci*, Nanotechnol*. 2012, **12***,* 439–445.
20. Q. Yu, H. Dong, X. Zhang, Y.X. Zhu, J.H. Wang, F.M. Zhang, X.J. Sun, *CrystEngComm.* 2018, **20***,* 3228–3233.
21. Y. Miyazaki, Y. Kataoka, Y. Kitagawa, M. Okumura, W. Mori, *Chem. Lett.* 2010, **39***,* 878–880.
22. P. C. Meenu, M. A. Sha, R. Pavithran, V. S. Dilimon, S. M. A. Shibli, *Int. J. Hydrogen Energy* 2020, **45**, 24582–24594.
23. X. Liu, X. Lv, H. Lai, G. Peng, Z. Yi, J. Li, *Photochem. Photobiol.* 2020, **96**, 1169–1175.